ISSN 1330-3651 (Print), ISSN 1848-6339 (Online) https://doi.org/10.17559/TV-20240519001615
Original scientific paper

Efficient Detection and Measurements of Bridge Crack Widths Based on Streamlined Convolutional Neural Network

Yingjun WU*, Junfeng SHI, Benlin XIAO, Hui ZHANG, Wenxue MA, Yang WANG, Bin LIU

Abstract: The automation of bridge disease detection necessitates the time-consuming, labor-intensive manual detection process and the limitations of traditional image segmentation methods, such as inadequate denoising effects and insufficient continuity in crack segmentation. This paper proposes a rapid detection and information feedback approach based on an enhanced Convolutional Neural Network (CNN) model to tackle these issues in bridge crack width measurement and information processing. To improve efficiency and accuracy in bridge safety monitoring, the training data is constructed by the bridge image library and network crack through the refined preprocessing and image segmentation techniques applied to these images, key features of cracks are identified and extracted to enhance the capability for crack identification. For crack assessment, the maximum internal tangent circle method is employed to accurately measure the width of bridge abutment cracks. The effectiveness of our model was verified through both fixed-point detection and Unmanned Aerial Vehicle (UAV) dynamic detection, ensuring comprehensive and accurate data collection. This dual validation strategy shows that our model substantiates the wide applicability across various scenarios, and the non-contact crack measurement technique achieves a precision of 0.01 mm, demonstrating the effectiveness and accuracy of this streamlined CNN model in accurately assessing crack width.

Keywords: convolutional Neural Networks; crack detection; crack measurement; image segmentation

1 INTRODUCTION

With the continuing problem of aging and deterioration of bridge structures worldwide [1], there is an urgent need to identify and diagnose existing bridge defects. Cracking is the most common defect in concrete structures, leading to problems such as water ingress, reinforcement corrosion, reduced durability, and loss of load-carrying capacity [2]. These potential risks affect the safety of the bridge structure and require crack detection throughout the life cycle of the bridge [3]. The monitoring of bridge health is essential to ensure transportation safety. Cracks pose a significant threat to the structural integrity of concrete bridges [4, 5]. Regular inspections and maintenance can mitigate the risk of structural failure during natural disasters like earthquakes or floods [6-9]. Measuring the width of bridge cracks plays a crucial role in assessing bridge safety. But traditional crack measurement methods relying on inspectors using rulers or magnifying glasses are time-consuming, cumbersome, and subjective in nature [10, 11]. Although crack detection systems based on fiber optic sensors, lasers, stereo imaging, ultrasound, and other technologies have been developed [12, 13]; these systems often come with high costs that make continuous real-time monitoring of bridge structural health unfeasible.

The researchers in the field of concrete crack image classification have made significant advancements in crack image recognition and segmentation [14], object detection [15][14], and image segmentation [16, 17]. Moreover, DCNN-based approaches have also been proposed for line detection tasks including edge detection [18, 19], contour detection [20], and boundary segmentation [21]. By layering convolutional sensory inputs, these sophisticated architectures effectively extract high-level features from low-level primitives. But there remains room for improvement in terms of the accuracy of edge processing specifically for cracks.

To address the challenge of achieving precise crack measurement and edge pixel refinement using existing techniques, the accuracy and clarity of crack recognition can be further enhanced by analysing the representation of cracks from two visual perspectives. From a global perspective, it is perceived as a thin, pixel-wide edge in an image due to its low contrast with the background. From a local perspective, it is identified as a line object with a specific width. Some scholars have proposed methods for the marginalization of image segmentation, with the first study of crack detection using image processing related to the intensity thresholding method due to its simplicity and efficiency [22]. Qu et al. demonstrated the identification and connection of linear crack targets through the application of basic mathematical morphological operations [23]. But excessive threshold settings were found to reduce the effectiveness of similar methods. Conversely, segmentation algorithms for edge detection are mainly based on local grayscale and gradient information to identify crack edges, and they can only be applied to crack maps with strong edge labels [24]. With the increase in image data size, several studies have explored the use of image processing and machine learning methods. Wang et al. [25] employed a support vector machine (SVM) to identify aircraft skin cracks, while Bray et al. [26]utilized neural network classification methods for identifying road defects. But, the identification of crack structures, distortions, and needle-like edges in bridge concrete cracks is not sufficiently clear and comprehensive due to numerous conditions and complex calculations. This process requires significant resources and exhibits slow processing speeds, resulting in inadequate accuracy when measuring crack widths. Therefore, preprocessing and analysis of image data are necessary to enhance the performance of the CNN neural network model.

The current quantitative analysis of crack hazard, including crack length, width, and depth, is inadequate [27]. Despite extensive research on image segmentation and crack recognition, limited progress has been made in analysing the crack width [28], and the preparation of image-based crack width measurements remains a challenge [29]. Therefore, accurate measurement of cracks is crucial for their prevention and to extend the service life of bridges after filtering noise, removing blur, and

segmenting the recognized images. Shan et al. [30] asserted that the type, quantity, width, and length of road cracks serve as indicators for assessing the early deterioration level of concrete structures. Luo et al. [31], in their study, examined crack edges in four directions based on the crack skeleton and adopted the minimum distance between two edges in these directions as the crack width. Although their approach performed well when idealizing cracks, it is important to note that in reality, the width tends to be measured as the straight-line distance between two edges perpendicular to the direction of crack expansion. Additionally, crack edges often exhibit irregular protrusions leading to asymmetry within the skeleton. The Hilditch thinning algorithm [32] effectively reduces distortions and needle-like edges. But, its complexity stems from numerous conditions, requiring significant computational resources and resulting in slow processing speed. Zhang and Suen [33] have made improvements to enhance the algorithm's processing speed; but it does not guarantee the thinning of a single pixel, struggles with accurately identifying bifurcation points, and still exhibits needle-like margins during the thinning process. Moreover, it lacks geometric meaning and accuracy for crack measurement applications.

The limitations of the aforementioned approaches contain: incomplete training samples, lack of image preprocessing leading to reduced accuracy in crack identification, and absence of a dual verification mechanism for data, resulting in a significant number of pixel errors [34]. Therefore, combined with the bridge image library and the network crack database, a unique and comprehensive training dataset has been constructed. Preprocessing and image segmentation techniques have been introduced for the comprehensive dataset, and the maximum inscribed circle method is utilized to precisely measure the width of bridge pier cracks for crack assessment. Additionally, a dual verification strategy, incorporating fixed point detection and drone dynamic detection, is proposed to ensure the effectiveness of the model and the comprehensiveness and accuracy of data collection.

The study is structured into several sections. Firstly, a concise introduction is provided on the network structure and algorithm principles of Convolutional Neural Networks (CNN). The captured crack image undergoes data enhancement and width measurement using an image segmentation method. The methodology introduces an improved model along with a segmentation approach that requires the desired image. In the experimental analysis, the enhanced CNN model is employed to identify and label cracks in an enhanced dataset while measuring the width of concrete cracks. Subsequently, a comparison is made between this approach and conventional crack detection methods to highlight their differences. Part five focuses on verifying the effectiveness of this method by identifying and measuring cracks on an actual bridge project, followed by comparing it with conventional crack measurement methods. Finally, a summary of related research findings concludes this study.

2 METHODOLOGY

In order to accurately measure the width of bridge cracks, a recognition technique based on Convolutional Neural Network (CNN) was employed. Firstly, high-definition photographs of the bridge cracks were captured using a non-contact method to obtain image data. Subsequently, the crack dataset underwent training with various features such as classification recognition, labelling, feature extraction, and image preprocessing and binarization in order to enhance the visibility of crack information. Following this, geometric characterization was applied to processed crack images and the maximum width of each crack was precisely calculated using the maximum tangent circle method for effective detection. To validate the effectiveness of this approach, both fixed-point measurement and UAV dynamic shooting were utilized for detecting bridge cracks in real-world projects, thus to determine the role of the method in identification of cracks in bridges (Fig. 1).

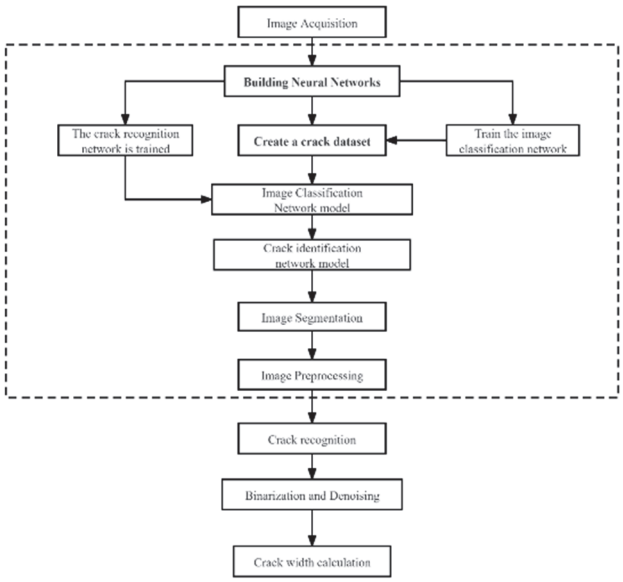

Figure 1 Flowchart of crack identification and extraction

2.1 Improved CNN Neural Network Model

Image crack feature extraction and classification are implemented by the proposed convolutional neural network model [35] in this paper. The network structure consists of 7 layers, including 4 convolutional layers and 3 fully connected layers, exhibiting a simple yet highly efficient design. Two of the convolutional layers are connected after the maximum pooling layer, while Dropout is applied to the two fully connected layers. This convolutional neural network employs smaller-sized convolutional kernels with step stride = 1, image padding = 1, and a size of 3 × 3 in all convolutional layers. Additionally, it utilizes pooling kernels with a step size of 2 and a size of 2 × 2 in all pooling layers to enhance detection accuracy. To further improve detection accuracy, the CNN model structure along with its flowchart is illustrated below (Fig. 2).

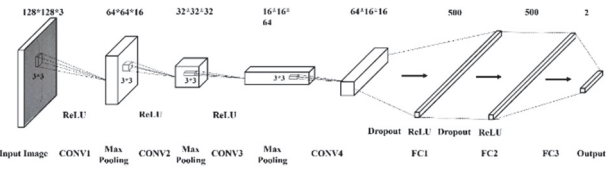

Figure 2 Simplify the CNN model structure

2.2 CNN Model Training

In optimizing point-to-point convolutional neural networks using transfer learning techniques, the cross-entropy loss function and adaptive moment estimation optimization function are selected, with a learning rate set to 0.01. The model is then implemented on the training dataset, tracking changes in real-time for both loss and accuracy of both training and validation sets. The number of iterations is predetermined while clearly defining concepts such as training loss and validation loss. Network weights are initialized through gradient clearing strategies while bias values remain fixed to maintain initial network stability. Sample batches from the training dataset are randomly drawn to obtain predictions via forward propagation; deviation between actual output and predicted value (i.e., loss value) is calculated to evaluate model performance. If the preset threshold for training error or maximum iteration limit has been reached, execution terminates; otherwise, it continues until completion. During backpropagation phase, gradient of loss function with respect to model parameters is calculated while updating network weights, thresholds, and losses accordingly; forward propagation validates model performance by calculating validation set losses which update average validation loss values (Fig. 3).

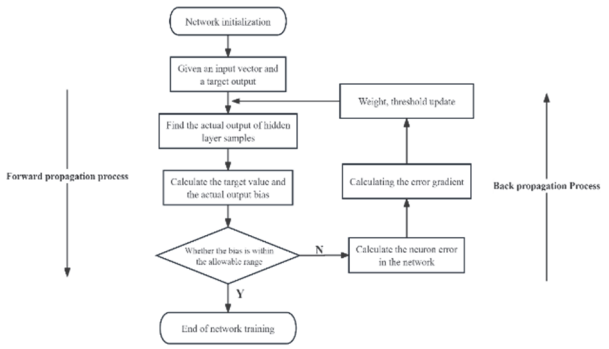

Figure 3 Neural network training process

2.3 Crack Target Extraction and Qualitative Measurements

The extraction of the target area is the basis of the crack detection algorithm, and the crack is extracted from the preprocesses crack image. The image segmentation algorithm will classify and analyze different regions in the image according to gray, color or geometric properties, and separate the crack region in the image from the background region. Finally, the extracted region was measured, the length, width, direction and other characteristic parameters of the region were quantitatively identified, and the information of all regions in the image in the region was displayed.

Edges are fundamental aspects of an image that exist between regions and play a crucial role in image segmentation. The edge detection method operates on the underlying assumption that the grayscale between adjacent regions in the image exhibits substantial shifts. Greyscale modifications in the information can usually be identified using the first-order derivatives of the excess value of the second-order derivative or the second-order derivatives of the zero-crossing. The gradient operator of the image is the first-order derivative operator. For a continuous image function, $f(x, y)$ can be represented as a vector to express the gradient [18, 19].

$$\nabla f(x,y) = [G, G] = \left[\frac{\partial f}{\partial x}\frac{\partial f}{\partial y}\right] \tag{1}$$

To further simplify the calculation:

$$|\nabla f(x,y)| = \left|\left[\left(\frac{\partial f}{\partial x}\right)^2 + \left(\frac{\partial f}{\partial y}\right)^2\right]\right|^{(\frac{1}{2})} \tag{2}$$

$$\varphi(x,y) = \arctan\left[\frac{\frac{\partial f}{\partial x}}{\frac{\partial f}{\partial x}}\right] \tag{3}$$

where:

$$\nabla_x = f(x,y) - f(x+1,y) \tag{4}$$

$$\nabla_y = f(x,y) - f(x,y+1) \tag{5}$$

After performing crack identification, labelling, image preprocessing, and binarization steps, the maximum width of bridge cracks was measured using advanced semantic segmentation techniques. Subsequently, their geometric features were further analysed. By employing the semantic segmentation method to delineate rectangular boxes around the cracks for highlighting their precise location and size, accurate calculation of the maximum crack width was achieved through the utilization of the maximum tangent circle method. These detections serve as a crucial foundation for conducting safety assessments on beam bridges. The following presents an overview of the crack width detection architecture.

The proposed method initially identifies the internal tangent circle within each crack location and subsequently determines the crack width based on the radius of this internal tangent circle, as illustrated in Fig. 4.

Let the radius of the inner tangent circle be R, then the radius maximum width $W_{\max}$ and average width W_{mean} of the crack are:

$$W_{\max} = 2\max\{R_i\} \tag{6}$$

$$W_{\text{mean}} = \frac{2\sum_{i=0}^{n} R_i}{n} \tag{7}$$

The images containing bridge cracks are annotated using semantic segmentation, and rectangular bounding boxes are utilized to precisely indicate the location and dimensions of the detected cracks.

Figure 4 Schematic diagram of the maximum tangent circle method

2.4 Crack Image Segmentation Algorithm

The introduction of operators [36, 37] enhances the effectiveness of the edge detection algorithm, thereby facilitating more efficient image segmentation. Notably, among these operators are the Roberts operator, Sobel operator, Prewitt operator, and Canny operator. Additionally, employing the Log operator with second-order derivatives yields significant improvements in edge detection.

The following figure compares these algorithms using the same crack image on MATLAB for detection, by comparing the different algorithms and analysing the image [37]; the Canny edge operator is used to threshold the image for segmentation processing. After this processing, the effect of noise on the crack image is less and thus the main contour of the crack is extracted more clearly.

After the bridge crack image has undergone light equalization processing, histogram equalization is employed to modify the grayscale of each pixel in the image by altering its histogram [38]. This process expands the range of grayscale values associated with a significant number of pixels (Those that contribute significantly to the overall picture) while compressing the range of grayscale values associated with a small number of pixels (i.e., those that have minimal impact on the picture). The objective is to enhance contrast, improve clarity, and achieve effective image enhancement.

After a series of enhancements to the image, the image is processed using iterative binarization to highlight the crack detection [37]:

1) Initial threshold setting. The image's minimum grey value $H_{\min}$ and maximum grey value $H_{\max}$ are determined, and the average value Have of both is used as the starting threshold value.

$$H_{ave} = \frac{H_{\min} + H_{\max}}{2} \tag{8}$$

2) Initial Image Segmentation. By setting an initial threshold, the image can be segmented into two subsets of grey level: C_1 and C_2.

$$\begin{Bmatrix} C_1 = \{f(x,y) \le H_{ave}\} \\ C_2 = \{f(x,y) > H_{ave}\} \end{Bmatrix} \tag{9}$$

3) Calculate the iterative threshold value, H:

$$H = \frac{\frac{1}{num(C_1)}\sum_{(x,y)\in C_1} f(x,y) + \frac{1}{num(C_2)}\sum_{(x,y)\in C_2} f(x,y)}{2} \tag{10}$$

4) Iteration and convergence, according to the calculated iteration threshold, repeat steps 2) to 4) until the threshold converges to a certain value or the number of iterations reaches a limited number of iterations. The flowchart of the iterative binarization algorithm and the effect diagram are shown below (Fig. 5).

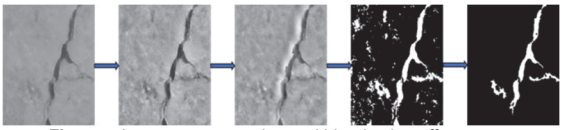

Figure 5 Image preprocessing and binarization effect

3 EXPERIMENT RESULTS & ANALYSIS

In this research, the crack images of the old bridge and the public crack dataset are collected. Firstly, an improved CNN model and the maximum inscribed circle method are utilized to measure the width of cracks on the bridge, in order to confirm the effectiveness of trained improved CNN model for concrete crack measurement. Meanwhile, in order to further validate the effectiveness of the approach in practical implementation, a case study was conducted utilizing fixed-point scanning photography and UAV dynamic photography methods to assess abutment cracks at Youyi Canal Crossing Bridge located in Xindian North Xiaojie, Xibeiwang Town, Haidian District, Beijing, China.

The Youyi Drain Crossing Bridge (Fig. 6), depicted in the image, was completed in 2014. This bridge features a prestressed concrete simply supported T-beam superstructure with a total length of 35.04 meters and a single span measuring 28.5 meters. The lateral layout consists of 10 center girders and 2 side girders, evenly spaced at intervals of 1.65 meters. The side girders extend externally by a length of 0.675 meters at their ends, while wet joints measuring 0.45 meters connect the girders to ensure structural integrity and load carrying capacity. High-strength C50 concrete materials were utilized for constructing the main girders, flange plates, diaphragm beams, and wet joints to enhance durability and strength. For the substructure design of this bridge, a pile-jointed cover girder type abutment was adopted using C35 concrete for abutment caps and ear back walls. Additionally, submerged C30 concrete was employed to cast the pile foundation supporting the bridge deck with a length reaching up to 33 meters.

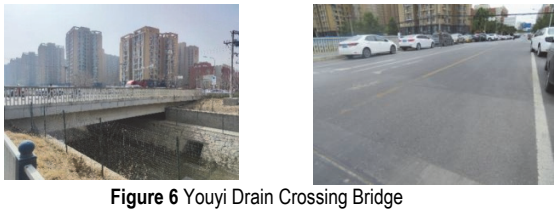

Figure 6 Youyi Drain Crossing Bridge

The Pytorch framework will be utilized to train an improved CNN neural network in order to enhance the accuracy of crack image recognition. During this process, a pre-trained network will serve as the foundation, while image enhancement techniques will be employed to further optimize the model's performance. Various transformations such as vertical and horizontal flipping,

rotation, and brightness adjustment will be applied to diversify the images, thereby enhancing the model's generalization ability.

3.1 Identification and Marking of Cracks

After applying image enhancement techniques and augmenting the dataset, the order of the data is randomized before splitting it into a training set and a test set. These sets are organized into two distinct folders: "positive samples" and "negative samples," ensuring comprehensive learning from various data features. The training set comprises 80% randomly chosen instances for effective model training and optimization purposes, while the remaining 20% is allocated as an evaluation test set to assess overall performance. Maintaining balance between positive and negative instances in both sets, an equal distribution of 200 images per category is included. Additionally, all images undergo uniform resizing procedures resulting in an approximate resolution of 128 × 128 pixels.

To improve the accuracy of crack width calculation, it is necessary to use high-resolution images due to the dense distribution of pixel points. Utilizing the original image for neural network prediction would result in a compression rate over 20 times, leading to a significant loss of crack details. Therefore, each crack image is divided into small cells with an approximate size of 128 × 128 using a horizontal and vertical overlap rate of 50% (Fig. 7). Subsequently, the model recognizes these crack images and automatically labels identified cracks in red color. The effectiveness of this recognition process is illustrated in Fig. 8 below.

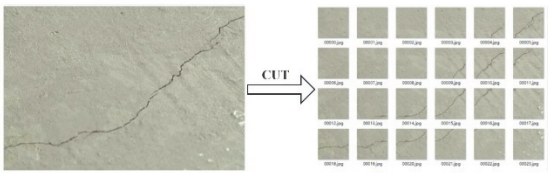

Figure 7 Image segmentation Sschematic

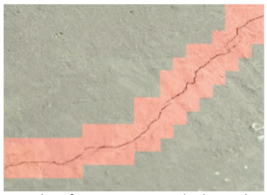

Figure 8 Schematic of concrete crack detection results

3.2 Comparison and Analysis of Crack Width Measurements

The improved CNN model was employed to recognize the crack images of a selected set of bridge cracks. Following the image recognition process conducted by the convolutional neural network on the crack-containing images, clear labels indicating both the crack area and the location of its maximum width can be observed in the images. Some examples of test result images are presented (Fig. 9a to Fig. 9f).

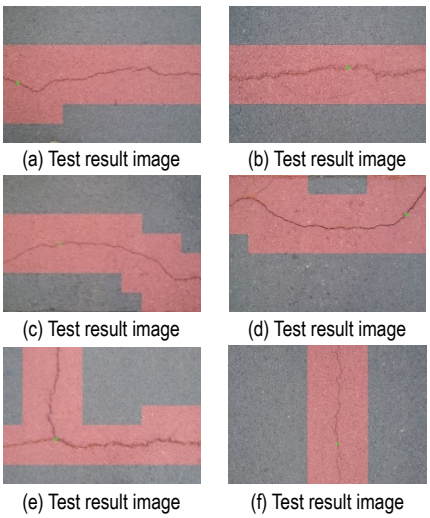

Figure 9 Image test results

The improve CNN model is utilized for precise identification of clear cracks and labelling the maximum position, enabling crack width detection in the image after network labelling. By comparing the detection results of the improved CNN recognition network with those obtained from a crack measuring instrument, we can determine any disparities between the test results and actual measurements. The comparison table and line graph illustrating the detected maximum crack widths using both methods are presented in Fig. 10a to Fig. 10e.

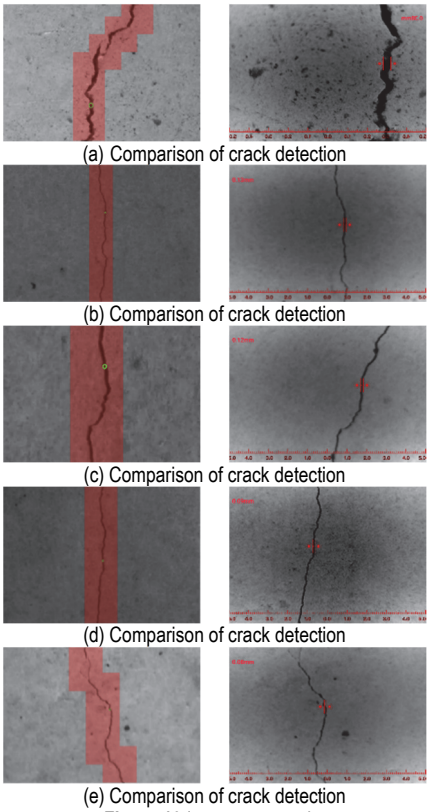

Figure 10 Image test results

A comparative analysis of Tab. 1 and Fig. 11 reveals a high level of consistency between the contactless measurement using the improved CNN model and the crack width gauge in terms of crack marking and maximum width calculation. The specific data indicates that there is

only a maximum error of 0.02 mm between the two methods, while the minimum error is zero. It should be noted that cracks 1 and 2 exhibit slightly larger results due to slight tilting of the crack width gauge and uncorrected vertical errors in the image. This observation underscores the significant advantage of utilizing an improved CNN model for eliminating human operation errors, further validating its superior measurement accuracy and enhanced crack detection capabilities.

Table 1 Crack width comparison table

Crack Number	Detection results based on improved CNN Model	Crack Width Gauge Measurement Results
1	0.36	0.38
2	0.14	0.13
3	0.12	0.12
4	0.09	0.09
5	0.07	0.08

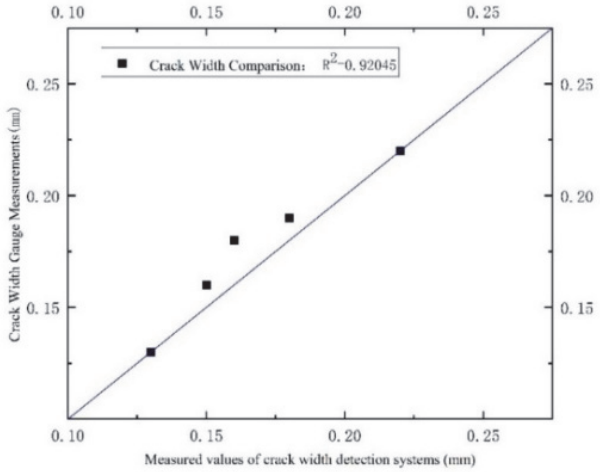

Figure 11 Comparison of maximum width of cracks

3.3 Practical Application of the Model

3.3.1 Spot Crack Detection

The bridge conducted a crack detection test by comparing and analyzing the cracks at five positions on the bridge side. Image-based technology, along with concrete girder bridge crack detection and monitoring equipment, as well as a crack width meter, were utilized for field application of crack detection on the bridge, as shown in Fig. 12.

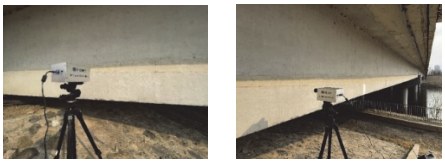

(a) (b)

Figure 12 Field survey picture

The control variable method is adopted to ensure the consistency of the crack width detection effect. The bridge cracks were measured using a scanner, with fixed angles and uniform light intensity at different positions. The processing results, based on improved CNN model detection and crack width meter, are shown in Fig. 13.

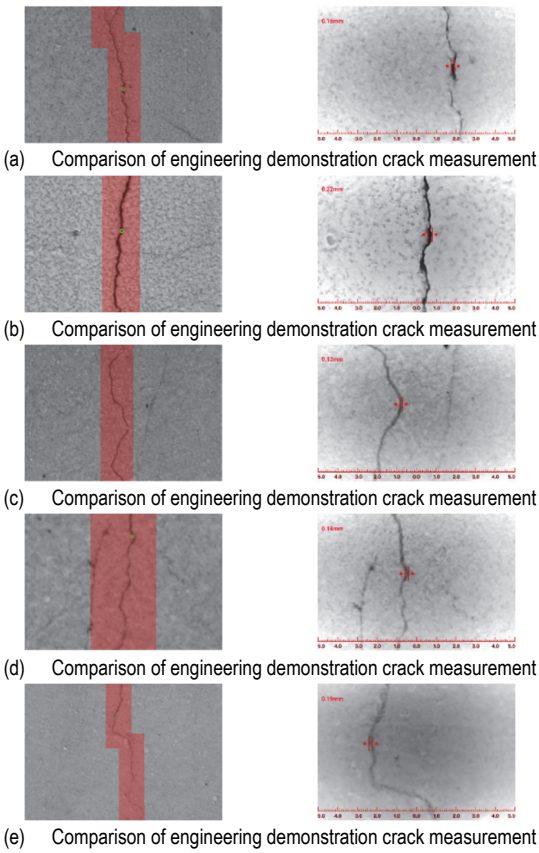

(a) Comparison of engineering demonstration crack measurement

(b) Comparison of engineering demonstration crack measurement

(c) Comparison of engineering demonstration crack measurement

(d) Comparison of engineering demonstration crack measurement

(e) Comparison of engineering demonstration crack measurement

Figure 13 Comparison of crack measurements for practical applications

3.3.2 Dynamic Crack Detection by Drones

The feasibility of this method in dynamic detection is demonstrated by utilizing a UAV to scan and detect cracks on the bridge pier. A combination of UAV imagery and an enhanced CNN model was employed to capture the comprehensive image of the beam bridge, enabling identification and measurement of 11 surface cracks. The crack analysis results are illustrated in Fig. 14 and Fig. 15.

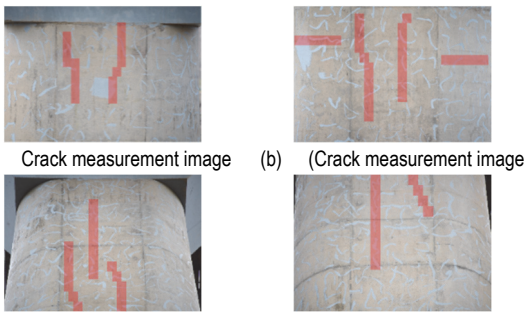

(a) Crack measurement image (b) (Crack measurement image

(c) Crack measurement image (c) Crack measurement image

Figure 14 Example of drone imaging cracks (a)~(c)

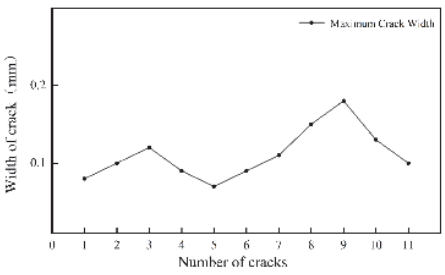

Figure 15 Maximum width of drone image crack example

The line graph illustrates the utilization of a drone as an image acquisition device, combined with convolutional neural network-based image recognition technology. This innovative approach enables rapid and efficient acquisition of information regarding surface cracks on girder bridges. It effectively addresses the challenge of detecting previously undetectable surface cracks in concrete girder bridges using traditional crack detection instruments. Additionally, this method offers convenient and highly accurate operation, making it suitable for practical applications in bridge inspection and maintenance.

4 DISCUSSION

The present research employs the streamed CNN model to establish an innovative image database, while utilizing the maximum inscribed circle method for crack width measurement. The experimental results demonstrate that the model effectively identifies the crack area and accurately determines the position of the maximum crack width, exhibiting a high level of consistency in both crack localization and width calculation. A comparison of the actual detection outcomes obtained from the enhanced CNN recognition network and crack measurement instrument with the results of the aforementioned methods revealed a maximum deviation of 0.02 mm between the two methods, with a minimum error of 0 mm. Therefore, it is evident that the occurrence of human error has been entirely eliminated. The efficacy of the model was validated through a case study on the Beijing Friendship Canal, employing fixed-point detection and UAV dynamic detection as dual verification techniques. The measurement accuracy achieved a remarkable 0.01 mm, exceeding the precision of traditional instruments for measuring crack width.

It should be noted, however, that the method presented in this paper does have certain limitations. Firstly, the application of deep learning to crack width measurement necessitates a substantial quantity of labelled data to prevent model overfitting and ensure accurate recognition by the model. There is too little variety of samples for training and deploying the model. The types of cracks included in the bridge crack dataset are relatively limited. In addition to vertical and lateral cracks, it is possible that other potential crack types may be present. It is important to note that the test does not consider image datasets of bridge cracks under complex interference backgrounds, despite supplementing the bridge crack dataset with field shooting and production data. Moreover, it is necessary to enhance the sensitivity to sample noise. The diversity of data samples can be expanded in the future to effectively identify and quantify measurements of various types of bridge distress.

5 CONCLUSION

This research methodology of deep learning is employed to facilitate non-contact recognition and measurement of cracks, leveraging an extensive database of crack images from old bridges as well as shared image data. The application of this approach leads to the following conclusions:

(1) The traditional CNN model used in this study has been enhanced and innovated to develop a highly efficient end-to-end crack detection model. By optimizing the network structure and adjusting parameters, this model demonstrates exceptional performance in recognizing bridge cracks and extracting their contours, thus significantly improving overall detection efficiency. Additionally, by integrating the maximum inscribed circle method into crack width measurements, we can ensure precise and reliable results.

(2) The intricate texture of the bridge surface, coupled with the challenging environmental conditions, poses significant obstacles to crack recognition. To address this challenge, advanced image enhancement techniques and iterative binarization algorithms are employed for preprocessing crack images. These techniques effectively accentuate the distinctive features of cracks while minimizing background noise interference, thereby substantially enhancing both accuracy and stability during model training.

(3) The maximum inscribed circle method is employed based on the improved model for crack measurement after identification and extraction. Extensive experimental validation was conducted in actual bridge projects to verify the effectiveness of the proposed method. A combination of fixed-point measurements and UAV dynamic measurements was utilized to compare and analyze the method with traditional bridge crack detection instruments. The test results demonstrate that the proposed method achieves a high accuracy of 0.01 mm in crack measurement, full proof of its potential and value in practical engineering applications.

By effectively applying deep learning techniques for crack detection in bridges, we can enhance the diversity of training data, improve the model's generalization capability, and thereby facilitate the widespread adoption of intelligent crack detection systems. Consequently, the implementation of this technology will facilitate the monitoring of bridge health and establish a more comprehensive and precise system for bridge health monitoring.

Acknowledgements

This study was supported by a research Grant number. 2022YFC3801700, Project "Key Technologies of cloud-edge-end Data Collaboration Mechanism and Integrated Modeling in Engineering Construction", supported by the National Key Research and Development Program Date Availability statement.

6 REFERENCES

[1] Lattanzi, D. & Miller, G. R. (2014). Robust automated concrete damage detection algorithms for field applications. *J. Comput. Civ. Eng.*, *28*(2), 253-262. https://doi.org/10.1061/(ASCE)CP.1943-5487.0000257

[2] Hoskere, V., Yasutaka, N., Tu A. H., & Spencer Jr., B. F. (2020). MaDnet: multi-task semantic segmentation of multiple types of structural materials and damage in images of civil infrastructure. *Journal of Civil Structural Health Monitoring,* (10)5 757-773. https://doi.org/10.1007/s13349-020-00409-0

[3] Du, Y., Pan, N., Xu, Z., Deng, F., Shen, Y., & Kang, H. (2021). Pavement distress detection and classification based on YOLO network. *Int. J. Pavement Eng,* 22(13), 1659-1672. https://doi.org/10.1080/10298436.2020.1714047

[4] Golewski, G. L. (2021). Evaluation of fracture processes under shear with the use of DIC technique in fly ash concrete and accurate measurement of crack path lengths with the use of a new crack tip tracking method. *Measurement*, *181*(2021), 109632. https://doi.org/10.1016/j.measurement.2021.109632

[5] Gong, Q., Zhu, L., Wang, Y., & Yu, Z. (2021). Automatic subway tunnel crack detection system based on line scan camera. *Struct Control and Health Monitoring, 28*(8). https://doi.org/10.1002/stc.2776

[6] Dong, C. Z. & Catbas, F. N. (2021). A review of computer vision–based structural health monitoring at local and global levels. *Struct Health Monitoring*, *20*(2), 692-743. https://doi.org/10.1177/1475921720935585

[7] Chen, Z., Huang, X., Yu, S., Cao, W., Dang, W., & Wang, Y. (2021). Risk analysis for clustered check dams due to heavy rainfall. *Int J Sedim Res, 36*(2), 291-305. https://doi.org/10.1016/j.ijsrc.2020.06.001

[8] Zhao, E. & Chengqing, W. (2021). Risk probabilistic assessment of ultrahigh arch dams through regression panel modeling on deformation behavior. *Structural Control and Health Monitoring*, *28*(5), e2716. https://doi.org/10.1002/stc.2716

[9] Proske, D. (2018). Comparison of dam failure frequencies and failure probabilities. *Beton-und Stahlbetonbau, 113*, 2-6. https://doi.org/10.1002/best.201800047

[10] Tang, Y., Allen, A. Z., Lei, L., Guolong, W., & Enhui, Y. (2021). Pixel-level pavement crack segmentation with encoder-decoder network. *Measurement*, *184*, 109914. https://doi.org/10.1016/j.measurement.2021.109914

[11] Mohan, A. & Sumathi, P. (2018). Crack detection using image processing: A critical review and analysis. *Alexandria engineering journal, 57*(2), 787-798. https://doi.org/10.1016/j.aej.2017.01.020

[12] Van Steen, C., Hussein, N., Els, V., & Martine, W. (2022). Acoustic emission source characterisation of chloride-induced corrosion damage in reinforced concrete. *Structural Health Monitoring, 21*(3), 1266-1286. https://doi.org/10.1177/14759217211013324

[13] Ye, Y., Shaowei, H., Xiangqian, F, & Jun, L. (2022). Effect of adhesive failure on measurement of concrete cracks using fiber Bragg grating sensors. *Optical Fiber Technology*, *71*, 102934. https://doi.org/10.1016/j.yofte.2022.102934

[14] Krizhevsky, A., Ilya, S., & Geoffrey, E. (2021). Hinton. Imagenet classification with deep convolutional neural networks. *Advances in neural information processing systems, 25*. https://doi.org/10.1145/3065386

[15] Girshick, R. (2015). Fast R-CNN. *Proc. IEEE Int. Conf. Comput. Vis.,* 1440-1448. https://doi.org/10.1016/j.yofte.2022.102934

[16] Long, J., Shelhamer, E., & Darrell, T. (2015). Fully convolutional networks for semantic segmentation. *Proc. IEEE Conf. Comput. Vis. Pattern Recognit.,* 3431-3440.

[17] Nassir, N., Joachim, H., William, M. W., & Alejandro, F. F. (2015). Medical Image Computing and Computer-Assisted Intervention - MICCAI 2015. *18th International Conference, Munich, Germany*. https://doi.org/10.1007/978-3-319-24574-4

[18] Xie, S. & Tu, Z. (2015). Holistically-nested edge detection. *Proc. IEEE Int. Conf. Comput. Vis.,* 1395-1403. https://doi.org/10.1109/CCV2015.164

[19] Liu, Y., Cheng, M. M., Hu, X., Wang, K., & Bai, X. (2017). Richer convolu- tional features for edge detection, in Proc. IEEE Conf. Comput. *Vis. Pattern Recognit.*, 5872-5881. https://doi.org/10.1109/CVPR.2017.622

[20] Shen, W., Wang, X., Wang, Y., Bai, X., & Zhang, Z. (2015). Deepcontour: A deep convolutional feature learned by positive-sharing loss for con- tour detection. *Proc. IEEE Conf. Comput. Vis. Pattern Recognit.*, 3982-3991. https://doi.org/10.1109/CVPR.2015.7299024

[21] Yang, J., Price, B., Cohen, S., Lee, H., & Yang, M. H. (2016). Object contour detection with a fully convolutional encoder-decoder network. *Proc. IEEE Conf. Comput. Vis. Pattern Recognit.*, 193-202. https://doi.org/10.1109/CVPR.2016.28

[22] Kamaliardakani, M., Sun, L., & Ardakani, M. K. (2016). Sealed-Crack Detection Algorithm Using Heuristic Thresholding Approach. *J. Comput. Civ. Eng.*, *30*, 04014110. https://doi.org/10.1061/(ASCE)CP.1943-5487.0000447

[23] Qu, Z., Lin, L., & Guo, Y. (2014). Algorithm of Image Crack Detection Based on Morphology and Region Extends. *Comput. Sci.,* 41, 297-300.

[24] Fan, Z., Chong, L., Ying, C., Jiahong, W., Giuseppe, L., Xiaopeng, C., & Di Mascio, P. (2020). Automatic crack detection on road pavements using encoder-decoder architecture. *Materials, 13*(13), 2960. https://doi.org/10.3390/ma13132960

[25] Wang, C., Xianfeng, W., Xin, Z., & Zhiyu, L. (2016). The aircraft skin crack inspection based on different-source sensors and support vector machines. *Journal of Nondestructive Evaluation, 35*, 1-8. https://doi.org/10.1007/s10921-016-0359-3

[26] Bray, J., Verma, B., Li, X., & He, W. (2006). A Neural Network based Technique for Automatic Classification of Road Cracks. *IEEE Xplore*, 907-912. https://doi.org/10.1109/IJCNN.2006.1716193

[27] Lee, J. S., Sung, H. H., Il, Y. C., & Yeongtae, C. (2020). Estimation of crack width based on shape-sensitive kernels and semantic segmentation. *Structural Control and Health Monitoring, 27*(4), e2504. https://doi.org/10.1002/stc.2504

[28] Cho, H., Yoon, H. J., & Jung, J. Y. (2018). Image-based crack detection using crack width transform (CWT) algorithm. *IEEE Access, 6*, 60100-60114. https://doi.org/10.1109/ACCESS.2018.2875889

[29] Munawar, H. S., Ahmed, W. A. H., Assed, H., Carlos, A. P. S., & Travis, W. S. (2021). Image-based crack detection methods: A review. *Infrastructures, 6*(8), 115. https://doi.org/10.3390/infrastructures6080115

[30] Shan, B., Zheng, S., & Ou, J. (2016). A stereovision-based crack width detection approach for concrete surface assessment. *KSCE Journal of Civil Engineering, 20*, 803-812. https://doi.org/10.1007/s12205-015-0461-6

[31] Luo, Q., Baozhen, G., & Qingguo, T. (2019). A fast adaptive crack detection algorithm based on a double-edge extraction operator of FSM. *Construction and Building Materials*, *204*, 244-254. https://doi.org/10.1016/j.conbuildmat.2019.01.150

[32] Thawonmas, R., Hirano, M., & Kurashige, M. (2006). Cellular automata and Hilditch thinning for extraction of user paths in online games. *Proceedings of the 5th ACM SIGCOMM Workshop on Network and System Support for Games, NetGames '06. Singapore*, 30-31 https://doi.org/10.1145/1230040.1230048

[33] Zhang, T. Y. & Suen, C. Y. (1984). A fast parallel algorithm for thinning digital patterns. *Commun. ACM, 27*, 236-239. https://doi.org/10.1145/357994.358023

[34] Dung, C. V. (2019). Autonomous concrete crack detection using deep fully convolutional neural network. *Automation in Construction*, *99*, 52-58. https://doi.org/10.1016/j.autcon.2018.11.028

[35] Ren, S., He, K., Girshick, R., & Jian, S. (2015). Faster r-cnn:Towards real-time object detection with regionproposal networksIl. *Advances In Neural InformationProcessing Systems,* 91-99. https://doi.org/10.1109/TPAMI.2016.2577031

[36] Yufei, L., Liu, J. F., Jianguo, N., et al. (2021). Review and prospect of structural surface crack recognition based on digital image method. *Chinese Journal of Civil Engineering, 54*(6), 20.

[37] Guojun, Y., Yahui, Q., & Xiuming, S. (2024). Review of bridge crack detection based on digital image technology.

Journal of Jilin University (Engineering and Technology Edition), 54(02), 313-332.
[38] Jiang, J., Zhang, Y., Xue, F., & Hu, M. (2006). Local Histogram Equalization with Brightness Preservation. *Acta Electronica Sinica, 34*(5), 861-866.

Contact information:

Yingjun WU
(Corresponding author)
School of Civil Engineering, Architecture and Environment,
Hubei University of Technology,
Wuhan 430068, China
E-mail: 102110959@hbut.edu.cn

Junfeng SHI
School of Civil Engineering,
Architecture and Environment.
Hubei University of Technology.
Wuhan 430068, China
E-mail: 592297026@qq.com

Benlin XIAO
School of Civil Engineering,
Architecture and Environment.
Hubei University of Technology.
Wuhan 430068, China
E-mail: 137878231@qq.com

Hui ZHANG
School of Civil Engineering,
Architecture and Environment,
Hubei University of Technolog,
Wuhan 430068, China
Key Laboratory of Health Intelligent Perception and Ecological Restoration of River and Lake, China
E-mail: zhhust@hbut.edu.cn

Wenxue MA
China Construction Industrial Engineering Industry Technology Research Academy Co, Ltd
Beijing 101300, China
E-mail: ma.wenxue@qq.com

Yang WANG
China Construction Industrial Engineering Industry Technology Research Academy Co, Ltd
Beijing 101300, China
E-mail: mawenxue@cscec.com

Bin LIU
China Construction Industrial Engineering Industry Technology Research Academy Co, Ltd,
Beijing 101300, China
E-mail: 861666137@qq.com